A Cell Simulator for optimizing the operation practices and the process control

Jacques Antille[1], René von Kaenel[2], Louis Bugnion[3]
1. Senior consultant, KAN-NAK Ltd.
2. CEO, KAN-NAK Ltd.
3. Project manager, KAN-NAK Ltd.
Corresponding author: rene.vonkaenel@kannak.ch

Abstract

The Hall-Heroult process can be described by a wide range of complex chemical and physical phenomena. Using MatLab-Simulink software, a mathematical model has been developed to solve the dynamic status of an aluminium reduction cell. Simulink provides a very powerful graphical user interface for building sub-models as block diagrams. The cell simulator determines various process interactions. The key operating parameters such as alumina concentration, bath temperature, ledge thickness, cell voltage and many others are computed as a function of time. Raw materials and process variations effects are predicted. The model can be used for improving operating strategies, can be implemented in the process control or can help at understanding the effect of various actions on the cell. Applications such as the variation of ledge thickness, specific energy, bath level, AlF_3 emissions are presented.

Keywords: Cell simulator; process control; process optimization; energy saving.

1. Introduction

Despite the fact that the Hall-Heroult process is based on a simple theory, there is a wide range of complex physical-chemical phenomena that must be taken into consideration when modeling the overall process. Many of these are dynamic, either periodic or transient and the dynamics of the process has important implications on process efficiency. Several dynamic cell simulators have been published with different objectives from increasing the understanding of the process to development and analysis of process control [1 – 6]. These simulators are using in-house programming. Contrary to this, the simulator described in this paper is based on MatLab-Simulink software, which is an open modelling system.

The objective of this work is to develop a mathematical model of a Hall-Heroult reduction cell as well as develop a better understanding of the reduction process itself. The effects of variations in operational parameters on the dynamical behavior of an aluminum reduction cell are predicted. Various couplings exist between the complex physiochemical phenomena. Compromises have to be made between simplicity and accuracy of the model. The most relevant aspects of the Hall-Heroult process are preserved. The cell simulator is structured in three main modules:

- Material balance model,
- Cell voltage model,
- Thermal balance model.

The three modules are then combined into one overall cell model which can be used for improving control strategies, cell operation as well as developing a predictive tool for the process itself. The model is not limited in the period of prediction. Operations such as anode change, tapping, alumina and aluminum fluoride feeding can be defined easily by the user. A period of 26 days can be simulated in less than 15 minutes. The simulation of one hour operation needs about 1 second computer time. The model can therefore be used online to help in process control strategies.

The cell simulator uses MatLab-Simulink software capabilities which integrate:

- Computation visualization programming of problems which are expressed in familiar mathematical notation,
- A graphical user interface (GUI) for building models as block diagrams, allowing you to draw models as you would with pencil and paper,
- A tool for simulating dynamics systems,
- Block diagram windows, in which models are created an edited by mouse driven command.
- Interactive graphical environment simplifying the modeling process, eliminating the need to formulate differential equations,
- Open modeling system to add new algorithms such as smoothing of cell resistance or anode effect detection.

2. Material balance module

The properties of the bath depend on the chemical composition of the electrolyte, so the dynamic change in the concentration of each chemical constituent involved is of great importance to the overall cell model. The mass conservation law for a system with a chemical reaction is:

Input + Generation = Output + Accumulation

2.1. Aluminum production rate

The aluminum electrolysis process is governed by Faraday's law of electrolysis and for aluminium can be expressed as:

$$\frac{dm_{Al}}{dt} = 9.321472 \cdot 10^{-8} I\eta \qquad (1)$$

m_{Al} Mass of aluminium produced at the electrode [kg]
I Current in the cell [A]
η Current efficiency [fraction]
t Time [s]

2.2 Carbon consumption rate

The aluminum (1) oxide is decomposed into aluminum and oxygen. The oxygen formed then reacts immediately with the carbon anode to carbon dioxide and carbon monoxide described by the two principle electrolysis equations:

$$2Al_2O_3 + 3C = 4Al + 3CO_2 \qquad (2)$$

$$Al_2O_3 + 3C = 2Al + 3CO \qquad (3)$$

Pearson and Waddington assumed that the loss in current efficiency is only due to the internal recombination of aluminum and carbon dioxide. By modifying the two principal equations with this assumption results in the modified electrolysis equation:

$$2\eta Al_2O_3 + 3C = 4\eta Al + 3(2\eta-1)\ CO_2 + 6(1-\eta)\ CO \qquad (4)$$

From the rate of aluminum produced and the electrolysis equation, the theoretical carbon consumption rate can be expressed as:

$$\frac{dm_C}{dt} = 3.11213 \cdot 10^{-8} I \quad (5)$$

Correspondingly, the production rate of carbon monoxide and carbon dioxide can be expressed by:

$$\frac{dm_{CO}}{dt} = 1.45154 \cdot 10^{-7} I(1-\eta) \quad (6)$$

$$\frac{dm_{CO_2}}{dt} = 1.140324 \cdot 10^{-7} I(2\eta - 1) \quad (7)$$

There are various additional loss mechanisms that contribute to the overall consumption, such as air and CO_2 burning of the anode as well as detachment of anode carbon particles as dust. The anode consumption rate is thus considerably higher in practice than expressed by Equation (5).

2.3. Alumina consumption rate

The alumina consumption is governed by the principal electrolysis equations. As for carbon, the alumina consumption can be expressed from the rate of aluminum produced and the modified electrolysis equations:

$$\frac{dm_{Al_2O_3}}{dt} = 1.76126 \cdot 10^{-7} I\eta \quad (8)$$

2.4. Cell emissions

A prebake cell emits around 20 kg of hydrogen fluoride (HF), 20 kg of particulate fluorides (i.e., in $NaAlF_4$) and 10 kg of sulfur dioxide (SO_2) per ton of aluminum. The fine particulate fluorides and gaseous hydrogen fluoride are of greatest concern in relation to the material balance, since fluorides are lost from the electrolyte. These are present in the anode gases as a result of gaseous fluoride evolution, particulate emission and entrainment of particulate materials. The subsequent sections concentrate on these.

2.4.1. Hydrogen fluoride evolution

The sources of the hydrogen H can be from the anode carbon or from moisture present in the air or in the alumina feed. Part of the hydrogen reacts with cryolite to produce hydrogen fluoride according to equation:

$$2Na_3AlF_6\ (l) + 3H_2\ (g) \rightarrow 2Al\ (l) + 6NaF\ (l) + 6HF\ (g) \quad (9)$$

The most favored reaction that water may undergo with the electrolyte constituents is that it may react with aluminum fluoride either in the electrolyte or in the emissions to produce fluoride. The reaction of the dissolved water with the electrolyte may be described in simplified form by:

$$2AlF_3\ (s) + 3H_2O\ (g) \rightarrow Al_2O_3\ (s) + 6HF\ (g) \quad (10)$$

According to Haupin [7], the total rate of the gaseous fluoride evolution in kilograms per ton of aluminum, can be estimated with the equation:

$$F_G = 1.4537 \cdot 10^7 \cdot e^{(0.78127R_b^2 - 3.1733 \cdot R_b - 8444/T_b)} \cdot \left(\frac{469 - 191 \cdot R_b}{P_b \cdot \%CE}\right) \cdot \left(\frac{C_{H_2O}}{37.44} + \frac{C_H}{21.5}\right)^{0.5} \cdot \left(\frac{C_{Al_2O_3}}{C^{max}_{Al_2O_3}}\right)^{-0.462} \quad (11)$$

R_b	Bath ratio (C_{NaF} /C_{AlF3})
P_b	Barometric pressure [kPa]
$\%CE$	Current efficiency [%]
T_b	Bath temperature [K]
C_{Al2O3}	Concentration of alumina [wt %]
C^{max}_{Al2O3}	Maximum solubility of alumina [wt %]
C_{H2O}	Concentration of H_2O in alumina feed mat. [wt %]
C_H	Concentration of hydrogen in the anode [wt %]

The production of electrolyte constituents due to cell fluoride emissions can then be approximated as follows in kilograms per ton of aluminum produced:

$$\Delta mAl = 0.011552F_G \quad (12)$$

$$\Delta mAl_2O_3 = 0.8726F_G \quad (13)$$

$$\Delta mAlF_3 = -1.473F_G \quad (14)$$

2.4.2. Vaporization

The tetrafluoroaluminate ($NaAlF_4$) is the most volatile species existing above cryolite-alumina melts. The vapor exists both as the monomer $NaAlF_4$ and as $Na_2Al_2F_8$, from the reaction of sodium fluoride with aluminum fluoride, according to:

$$NaF + AlF_3 \rightarrow NaAlF_4 \quad (15)$$

Vaporization is a significant factor when a driving force for removing the electrolyte vapors from the cell is present. In an operating cell this is provided by the gases from the anodes, which are mostly carbon dioxide and carbon monoxide. The rate of loss of vapors is thus dependent on the saturation vapor pressure. The total vapor pressure PT in [kPa] which is equal to the sum of the partial pressures of the individual gases can be expressed as a function of bath composition and temperature by equation [7]:

$$\log(P_T) = B - A/T_b$$

where :

$$A = 7101.6 + 3069.7R_b - 635.77R_b^2 + \frac{764.5 \cdot C_{Al_2O_3}}{1 + 1.0817 \cdot C_{Al_2O_3}} + 13.2C_{CaF_2} \quad (16)$$

$$B = 7.0174 + 0.6844R_b - 0.08464R_b^3 + \frac{1.1385 \cdot C_{Al_2O_3}}{1 + 3.2029 \cdot C_{Al_2O_3}} + 0.0068C_{CaF_2}$$

Assuming that the transpiring gases are saturated with vapor, the rate of fluoride evolution in kilograms per ton of aluminum, due to particulate emissions resulting from volatilization given by Haupin [7], can be approximated by:

$$F_{VP} = \frac{2040}{\eta} \cdot \frac{P_m + 2P_d}{P_b} \tag{17}$$

Where P_b is the barometric pressure and P_m and P_d are the partial pressure of the monomer and dimer respectively, given by:

$$P_m = \frac{\sqrt{1 + 4K \cdot P_T} - 1}{2K} \ (kPa) \tag{18}$$

$$P_d = P_T - P_m \ (kPa) \tag{19}$$

Where (*k*) is the dimensionless equilibrium constant for dimerization, given by:

$$K = exp(\frac{-21414}{T_b} + 15.6) \tag{20}$$

Finally one can express the consumption of electrolyte constituents due to particulate in kilograms per ton of aluminum as:

$$\Delta mNaF = -0.5525 F_{VP} \tag{21}$$

$$\Delta mAlF_3 = -0.105 F_{VP} \tag{22}$$

2.4.3. Entrainment of particulate materials

The mechanism when liquid droplets or solid particulates are entrapped in a flowing gas is known as entrainment. Haupin developed an empirical model for estimating the rate of fluoride evolution due to entrainment [7]:

$$F_E = \frac{1}{\%CE} \cdot (-17030 + 29800 \cdot R_b - 13000 \cdot R_b^2 + 67 \cdot C_{Al_2O_3} \\ -173 \cdot \tau - 0.3896 \cdot \tau^2 + 141.6 R_b \cdot \tau) \tag{23}$$

where: $\tau = T_b - 1243$

The total fluoride emission will thus become:

$$F_T = F_G + F_{VP} + F_E \tag{24}$$

From the fluoride loss and by assuming that the concentration of the slowly consumed constituents remains constant as before, the consumption of electrolyte constituents due to entrainment can be approximated by proportional calculations as follows, in kilograms per tonne of aluminum.

$$\Delta mAlF_3 = -1.473 C_{AlF_3} \cdot F_E \cdot f_F^{-1} \tag{25}$$

$$\Delta mNaF = -2.210 C_{NaF} \cdot F_E \cdot f_F^{-1} \tag{26}$$

$$\Delta mAl_2O_3 = -C_{Al2O3} \cdot \Delta M \cdot f_F^{-1} \quad (27)$$

Where f_F is the fraction of the electrolyte that is made up of fluoride compound and ΔM is the total mass change in the fluoride compound. Assuming that alumina is the only constituent that is not a fluoride compound,

$$f_F = (100 - C_{Al2O3}) \quad (28)$$

Neutralization of sodium and calcium oxide in alumina

One of the key factors for obtaining optimal aluminium production efficiency is to maintain the bath composition as stable as possible around specified target values. Usually the concentration of AlF_3 is kept from 10 % to 13 %. There are two basic oxides entering the cell together with alumina: Na_2O and CaO. They neutralize AlF_3 in the bath according to equations:

$$3Na_2O + 4AlF_3 \rightarrow 2Na_3AlF_6 + Al_2O_3 \quad (29)$$

$$3CaO + 2AlF_3 \rightarrow 3CaF_2 + Al_2O_3 \quad (30)$$

The first reaction produces cryolite and the second reaction forms CaF_2. The aluminium fluoride must be regularly added into the cell to readjust bath chemistry back to the targets. The AlF_3 addition rate is well predictable and depends on the alumina composition and scrubber efficiency. Another factor influencing the AlF_3 demand is the sodium content of the cathodes. Depending on the cathode status, the AlF_3 feed rate may be below the prediction because part of the sodium provided by the alumina is absorbed into the cathode in the early months of the cathode life.

2.6. Corrective fluoride additions

The amount of fluoride required for correcting the electrolyte composition is determined by the bath ratio which is the mass ratio of NaF to AlF_3. Another obvious reason for corrective additions is to maintain sufficient electrolyte volume. To increase the ratio, sodium fluoride is added to the electrolyte in the form of sodium carbonate (Na_2CO_3), which reacts with aluminum fluoride to form sodium fluoride (NaF), according to the reaction:

$$3Na_2CO_3 + 2AlF_3 \rightarrow 6NaF + Al_2O_3 + 3CO_2 \quad (31)$$

Sodium also enters the cell as impurity in alumina, sodium oxide Na_2O, which reacts with aluminum fluoride to form sodium fluoride:

$$3Na_2O + 2AlF_3 \rightarrow 6NaF + Al_2O_3 \quad (32)$$

Adding aluminum fluoride also reduces sodium deposition, since excess AlF_3 reacts with sodium to form cryolite, according to the reaction:

$$AlF_3 + 3NaF \rightarrow Na_3AlF_6 \quad (33)$$

2.6. Alumina feeding

The alumina feed algorithm is based on the process control algorithm and depends on the technology. It is normally based on a demand feed strategy analyzing the voltage or calculated bath resistance curve from the voltage. Figure 1 shows a typical dependence of the voltage as function of the alumina concentration.

The anode effect detection is also integrated in the alumina control model and takes place when the alumina reaches a critical low value.

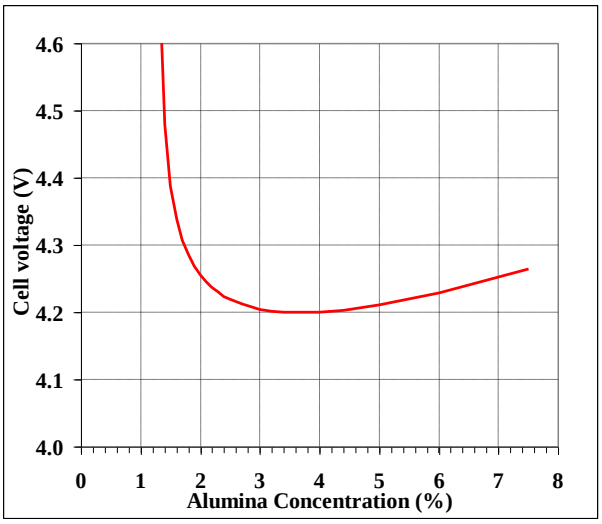

Figure 1. Cell voltage as a function of alumina concentration.

2.7. Alumina Dissolution

The alumina dissolution is a process by itself. Let us just mention that two specific time constant are used in the model associated to a fast and slow dissolution both following the dissolution equations:

$$\frac{dC}{dt} = -k_i \cdot C \qquad i = 1, 2 \qquad (34)$$

2.8. Total Material consumption and production

Normally, the only additives used in the electrolyte are aluminum fluoride AlF_3 and sodium carbonate Na_2CO_3, thus neither MgF_2 nor LiF are used. Calcium fluoride enters the bath as an impurity in the feed material and its proportion is sufficient to maintain the CaF_2 balance, thus no corrective additions are required. There are two main considerations for the neutralization: AlF_3 depends on the added mass of Al_2O_3 and its quality.

3. Properties of the Electrolyte

The physical properties of the electrolyte are strongly influenced by its composition and temperature. In the following, expressions for various properties involved in modeling the aluminum reduction cell are given.

3.1. Density

Several empirical equations have been published for calculating the density of the molten electrolyte. The empirical relationship given by Haupin is used in our simulator [8]:

$$\rho_{EL} = 10^5/(\frac{C_{Na_3AlF_6}}{3.305 - 0.000937 \cdot T_b} + \frac{C_{AlF_3}}{1.987 - 0.000319 \cdot T_b + 0.094 \cdot C_{AlF_3}} + \frac{C_{CaF_2}}{3.177 - 0.000391 \cdot T_b + 0.0005 \cdot C_{CaF_2}^2} + \frac{C_{Al_2O_3}}{1.449 + 0.0128 \cdot C_{Al_2O_3}} + \frac{C_{MgF_2}}{3.392 - 0.000524 \cdot T_b - 0.01407 \cdot C_{MgF_2}} + \frac{C_{Lif}}{2.358 - 0.00049 \cdot T_b})[kg/m^3] \quad (35)$$

Where T_b is bath temperature in kelvin. The density of the electrolyte must be below the density of liquid aluminum, for it to float on top of the metal pad. To reduce the mixing between the electrolyte and the metal pad, it is thus desirable to have a maximum difference in density. From the above equation the theoretical density of the electrolyte at 960 °C was found to be 2 113 kg/m^3. For comparison, the density of molten aluminum is close to 2 305 kg/m^3.

3.2. Viscosity

The viscosity of the electrolyte influences several hydrodynamic processes in the cell: movement of metal droplets in the electrolyte, dissolution and sedimentation of alumina particles, release of the gas bubbles from the anode surface. A simplified equation for the viscosity of the electrolyte is given by Grjotheim and Welch [9]:

$$\mu_{EL} = 11.557 - 9.158 \cdot 10^{-3} \cdot (T_b - 273) - 1.587 \cdot 10^{-3} \cdot C_{AlF_3} + (-2.049 \cdot 10^{-3} + 1.853 \cdot 10^{-5} \cdot (T_b - 1273)) \cdot C_{AlF_3}^2 - 2.168 \cdot 10^{-3} \cdot C_{Al_2O_3} + (5.925 \cdot 10^{-3} - 1.938 \cdot 10^{-5} \cdot (T_b - 1273)) \cdot C_{Al_2O_3}^2 [mPa \cdot s] \quad (36)$$

3.3. Alumina solubility

The maximum amount of alumina that can be dissolved in the electrolyte depends on both the electrolyte composition and temperature. The maximum alumina solubility can be expressed by the following equation, given by Skybakmoen [10]:

$$C_{Al-2O_3}^{max} = A \cdot \left(\frac{T_b - 273}{1000}\right)^B \quad (37)$$

where:

$$A = 11.9 - 0.062 \cdot C_{AlF_3} - 0.0031 \cdot C_{AlF_3}^2 - 0.20 \cdot C_{CaF_2} - 0.50 \cdot C_{LiF} - 0.30 \cdot C_{MgF_2} + \frac{42 \cdot C_{AlF_3} \cdot C_{LiF}}{2000 + C_{AlF_3} \cdot C_{LiF}}$$

$$B = 4.8 - 0.048 \cdot C_{AlF_3} + \frac{2.2 \cdot C_{LiF}^1 .5}{10 + C_{LiF} + 0.001 \cdot C_{AlF_3}^3}$$

When the concentration of alumina reaches the maximum alumina solubility, the electrolyte becomes saturated with alumina, and all excess alumina sinks to the bottom of the cavity, where it can form sludge. From the above equation and typical values related to the bath composition, the theoretical maximum alumina solubility of the electrolyte at 960 °C was found to be approximately 8 wt%.

3.4. Aluminium solubility

The tendency for metal to dissolve in the electrolyte is the primary cause for the lowering cell current efficiency. The lower the metal solubility, the higher resulting current efficiency. Hence the selection of the electrolyte composition is influenced by the need to ensure the metal solubility minimization, while at the same time ensuring that the melting point is low, since the metal solubility is strongly dependent on temperature. Based on correlation of measurements, the aluminum solubility can be expressed by the following equation [9]:

$$log(C_{Al}^{max}) = 1.8251 - \frac{0.2959}{R_{bath}} - \frac{3429}{T_b} - \frac{0.0339 \cdot C_{Al_2O_3}}{C_{Al_2O_3}^{max}} - 0.0249 \cdot C_{LiF} - 0.0241 \cdot C_{MgF_2} - 0.0381 \cdot C_{CaF_2} \quad (38)$$

From the above equation and typical values related to the bath composition, the theoretical maximum aluminum solubility of the electrolyte at 960 °C was found to be approximately 0.034 wt%.

4. Current efficiency

The internal recombination of aluminum and carbon dioxide is the main cause of the difference between the actual quantity of aluminum produced and the theoretical quantity stated by Faraday's law of electrolysis. The current efficiency can be estimated by Lillebuen model [11]:

$$\%CE = 100(1 - \frac{r_m}{r_{Al}}) = 100(1 - \frac{3Fr_m}{I}) \quad (\%) \quad (39)$$

Where r_m, r_{Al} is the ratio of the metal transfer through the bulk of the electrolyte and the theoretical rate of aluminum production, F is the Faraday constant and I the cell current. In order to fit plant data with better accuracy, our model is also using Solli's model, based on experimental and theoretical studies. The details of the work can be found in References [12 - 14]. The authors are considering the average of both theories.

5. Energy balance

The aluminum reduction process requires energy to keep the electrolyte at the reaction temperature and to produce aluminum, which is furnished as electric energy. The authors cannot develop the equations in the frame of this paper but would like to summarize the important elements imbedded in the model:
Enthalpy of reaction per mol of aluminum for the primary and re-oxidation reactions is [15]:

$$\Delta H_{react} = \frac{1}{2} \cdot \Delta H_f(Al_2O3) - \frac{3}{4}(2 - \frac{1}{\eta}) \cdot \Delta H_f CO_2 - \frac{3}{2}(\frac{1}{\eta} - 1) \cdot \Delta H_f(CO) \quad (40)$$

$$\Delta H_f(Al_2O_3) = 1692.44 - 0.011235 \cdot (T_b - 1100) \quad [KJ/mol] \quad (41)$$

$$\Delta H_f(CO_2) = 394.84 + 0.002095 \cdot (T_b - 1100) \quad [KJ/mol] \quad (42)$$

$$\Delta H_f(CO) = 112.59 + 0.00642 \cdot (T_b - 1100) \quad [KJ/mol] \quad (43)$$

where T_b is bath temperature in kelvin.

Enthalpy of heating the reactants and bath additives as well as enthalpy of alumina dissolution must be taken into account [15]:

$$H_{\gamma\to\alpha} = [\Delta H_f(\alpha) - \Delta H(\gamma)] \cdot c_\gamma(\%) \quad [\frac{kJ}{mol}] \tag{44}$$

$\Delta H_f(\alpha)$ Heat of formation for alumina in alpha phase (- 1675.69 kJ/mol),

$\Delta H(\gamma)$ Heat of formation for alumina in gamma phase (- 1656.86 kJ/mol),

$c_\gamma(\%)$ Concentration of gamma-phase alumina (wt%).

In steady state, the enthalpies of these reactions can be agglomerated, including the heating up of alumina and carbon and alumina dissolution. The overall enthalpy to make aluminium can be expressed with equivalent voltage to make aluminum. Calculated for the summary reaction which includes the primary reduction reaction with alpha alumina and the metal re-oxidation, with raw materials entering at 25 °C and reacting at electrolyte temperature T_b, the equivalent voltage to make aluminum as a function of temperature is [16]:

$$V_{Al} = 0.450 + 3.110\times10^{-5}T_b + \left[1.4316 - 0.03252(1-\varepsilon) + 2.255\times10^{-4}T_b\right]\eta \tag{45}$$

where: V_{Al} Voltage equivalent of enthalpy to make aluminum [V]

T_b Bath temperature [°C]

η Current efficiency, fraction

ε Fraction of alpha-alumina in alumina.

The internal heat (net heat) in the cell is then:

$$Q_{\text{int}} = \left(V_{cell} - V_{external} - V_{Al}\right) I \tag{46}$$

where: Q_{int} Cell internal heat [kW],

V_{cell} Cell voltage [V],

$V_{external}$ External voltage drop (the one outside the cell boundary, chosen for heat balance) [V],

I Current [kA].

This heat has to be lost from the cell through the cell boundaries, comprising all surfaces and solid connections to the outside of the cell by conduction, convection and radiation.

Auxiliary processes are also taken into account. The reaction enthalpies of these are [15]:

Chemical reaction	Enthalpy of reaction [kJ/mol]
$Na_3AlF_6(l) + 3/2H_2(g) \longrightarrow Al(l) + 3NaF(l) + 3HF(g)$	$\Delta H_{react} = -793.26 + 0.1258 \cdot T_b$
$2AlF_3(s) + 3H_2O(g) \longrightarrow Al_2O_3(s) + 6HF(g)$	$\Delta H_{react} = -324.03 + 0.07591 \cdot T_b$
$NaF + AlF_3 \longrightarrow NaAlF4$	$\Delta H_{react} = -895.21 + 0.93468 \cdot T_b$
$S + 2CO_2 \longrightarrow SO_2 + 2CO$	$\Delta H_{react} = -210.9 + 0.00748 \cdot T_b$
$3Na_2CO_3 + 2AlF_3 \longrightarrow 6NaF + Al_2O_3 + 3CO_2$	$\Delta H_{react} = -24.784 + 0.14984 \cdot T_b$
$AlF_3 + 3NaF \longrightarrow Na_3AlF_6$	$\Delta H_{react} = -169.3 + 0.09972 \cdot T_b$
$3Na_2O + 2AlF_3 \longrightarrow 6NaF + Al_2O_3$	$\Delta H_{react} = -844.58 - 0.18601 \cdot T_b$

where T_b is bath temperature in kelvin.

In a dynamic simulator, such as the one presented here, the heat capacitance of the cell materials and the ledge freezing and melting processes are included; they play key role on thermal state of the metal and electrolyte as a function of time and of pot operation events. The bath chemistry changes, which impacts electrical conductivity of the bath and cell voltage. Also the heating up of materials and alumina dissolution are treated separately from enthalpies of reactions since the additions of these materials are batch-wise, however frequent.

In the simulator, all types of events such as metal tapping, beam raising, current increase and feedings can be scheduled. The alumina feeding is of course of prime importance as it is used to control the bath voltage. It can be easily modified in the simulator to reflect the exact algorithms used for any particular smelter. Same remarks apply for the aluminium fluoride, calcium fluoride or any desired addition.

In the simulator output, the total heat loss is divided into shell bottom, side metal level, side bath level, side top, ends, collector bars, stubs and top heat losses.

6. Cell voltage model

The cell voltage is one of the most important operating parameters in aluminum reduction cells, and is often the only parameter measured in real time. Cell voltage is closely related to alumina concentration in the electrolyte, bath temperature and anode-to-cathode distance (ACD), which is adjusted by anode beam movements, and is thus generally, one of the bases for computer control of the Hall-Heroult process. The total cell voltage is composed of two different parts:

- Decomposition voltage or back electromotive force (back EMF), which consists of equilibrium potential and overvoltages, required for the decomposition of alumina.
- Ohmic voltage drops due to the resistance of various sections in the cell.

A comprehensive analysis of cell voltage components is given in [17].

7. Application

The cell is described by a set of over 300 parameters. This defines the cell geometry, the operating procedures and materials properties. Each parameter can be modified to analyze its impact on the process. Figure 2 shows a set of output from the model. After 8 hours one anode is changed, after 22 hours tapping is imposed to the cell. The analysis can be performed over a full anode cycle and beyond (more than 30 days). The feeding cycles are based on a “demand feed” algorithm in which the fast feeding is triggered by the slope (the rate of change) of the cell electrical resistance curve. A current fluctuation is imposed to the model (not compulsory) to simulate the rectifier fluctuations. As all formulas are somehow impacted by the current, it helps validating the smoothing algorithms needed to control the process fluctuations.

Figure 3 shows bath resistance, current efficiency and energy consumption for the analysed period. The high frequency signals result from the noise level imposed on the current.

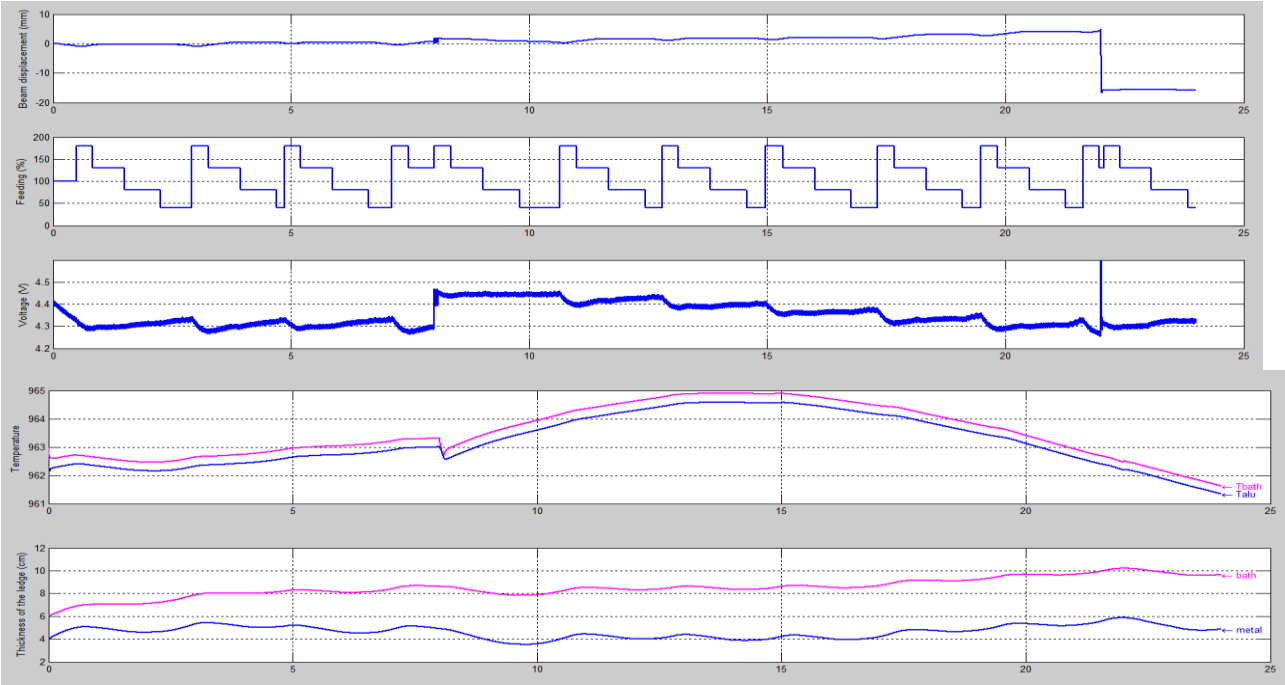

Figure 2. 24-hour plot of the beam displacements, feeding rate in % of nominal feed, cell voltage, bath and metal temperature and ledge at metal and bath level..

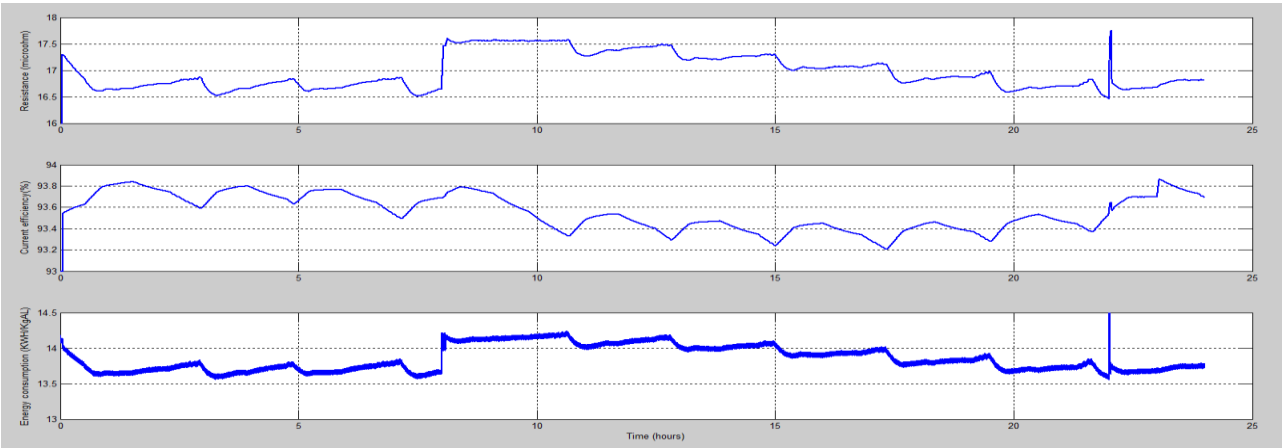

Figure 3. 24-hour plot of the bath resistance, current efficiency and energy consumption.

There are many more plots analyzing the energy balance, the bath chemistry and any desired parameter as function of time. Predictions were validated with measurements.

8. Conclusions

A sophisticated cell simulator has been developed using MATLAB-SIMULINK software. The software is fully open and can be easily modified to implement each plant alumina and aluminum fluoride feeding strategies or other specificities. It highlights how heat losses, current efficiency and other key operating parameters fluctuate during the day. It can be used to optimize the process.

9. References

1. Vanderlei Gusberti et al., Modeling the mass and energy balance of different aluminium smelting cell technologies, Light Metals 2012, pp 929-934.
2. Vanderlei Gusberti, Modelling the mass and energy balance of aluminium reduction cells, Dissertation (2014), University of New South Wales, Sydney, Australia.
3. M Dupuis, Simulation of the Dynamic Response of Aluminum Reduction cells Light Metals 1997, pp 443-447.
4. M.P. Taylor, W.D. Zhang, V. Wills, S. Schmid, A dynamic model for the energy balance of an electrolysis cell Trans IChemE, Vol. 74, Part A, November 1996, p. 913.
5. P. Biedler, Modeling of an Aluminium Reduction Cell for the Development of a State Estimator, Dissertation (2003), Morgantown, West Virginia.
6. S.W. Jessen, Mathematical Modeling of a Hall Héroult Aluminium Reduction Cell, Dissertation (2008), Technical University of Denmark.
7. W.E. Haupin, Production of aluminum and Alumina, John Wiley & Sons, Chichester, 1987.
8. W.E. Haupin, Chemical and Physical Properties of the Electrolyte, in Production of Aluminum and Alumina, Critical Reports on Applied Chemistry, A.R. Burkin [Ed], John Wiley & Sons, Chichester, 1987,Vol.20, pp 85-119.
9. Kai Grjotheim and Barry J. Welch, Aluminium Smelter Technology, 2nd Edition, Aluminium-Verlag, Düsseldorf, 1988.
10. Kai Grjotheim et al., Aluminium Electrolysis, 2nd Edition, Aluminium-Verlag, Düsseldorf, 1982.
11. W.E Haupin, Current Efficiency in Production of Aluminum and Alumina, Critical Reports on Applied Chemistry, A.R. Burkin [Ed], John Wiley & Sons, Chichester, 1987,Vol. 20, pp 134-149.
12. A. Sternen, P.A. Solli, An electrochemical current efficiency model for aluminium electrolysis, Journal of Applied Electrochemistry, 26 (1996), pp 187-193.
13. P.A. Solli, T. Eggen, E. Skybakmoen, Current efficiency in the Hall-Heroult process for aluminium electrolysis: experimental and modelling studies, Journal of Applied Electrochemistry, 27 (1997), pp 939-946.
14. A. Sternten and P.A. Solli, Cathodic process and cyclic redox reactions in aluminium electrolysis cells, Journal of Applied Electrochemistry, 25(1995), pp 809-816.
15. Jomar Thonstad et al., Aluminium Electrolysis, 3rd Edition, Aluminium-Verlag, 2001.
16. Abdalla Al Zarouni et al., Energy and mass balance of DX+ reduction cells, 31st International Conference of ICSOBA, 19th Conference, Aluminium Siberia, Krasnoyarsk, Russia, September 4 – 6, 2013, pp 494-498.
17. W. E. Haupin, Interpreting the components of cell voltage, Light Metals 1998, pp 531-537.